Code Orthogonality for Wideband CDMA Systems With Multiple Transmit Antennas

Mythri Hunukumbure, Ben Allen, *Senior Member, IEEE*, and Mark A. Beach, *Member, IEEE*

***Abstract*—Code orthogonality is a useful indicator in determining the performance of the synchronous downlink of third-generation Universal Mobile Telecommunication System (UMTS) Terrestrial Radio Access systems. In this paper, previous work on quantifying code orthogonality for single-antenna [or single-input single-output (SISO)] links is extended to fixed beamforming and transmit diversity schemes. Code orthogonality estimates from real measured channel data are extracted for typical outdoor radio environments. The results indicate that the spatial conditioning of fixed beamforming radio channels generally improves code orthogonality. In contrast, full code-rate transmit diversity schemes degrade code orthogonality.**

***Index Terms*—Code orthogonality, fixed beamforming, space-time block codes (STBC), transmit diversity, wideband code-division multiple access (WCDMA).**

I. Introduction

AFTER a decade of research and standardization, the third generation (3G) of mobile communications has now become a commercial reality. Yet, certain aspects within 3G need further research and refinement before they can be fully incorporated into operational 3G networks. The High Speed Downlink Packet Access (HSDPA) scheme [1] and its uplink version (High Speed Uplink Packet Access) are notable examples. It was originally anticipated that the orthogonal variable spreading factor (OVSF) codes used in wideband code-division multiple access (WCDMA) [1] would nullify the intracell interference in the synchronous downlink. However, it soon became evident that the delay dispersive radio channels would partially destroy the OVSF code orthogonality, resulting in a corresponding increase in intracell interference. Several research papers in recent years have quantified this loss in code orthogonality for single-transmitter-to-single-receiver [or single-input–single-output (SISO)] radio links [2]–[5].

Manuscript received March 18, 2005; revised March 23, 2006, January 25, 2007, and February 15, 2007. This work was supported in part by the Higher Education Funding Council for England Joint Research Equipment Initiative 1998 and in part by OFCOM's U.K. Spectrum Efficiency Scheme. The work of M. Hunukumbure was supported by the ORS scheme and the University of Bristol scholarship during his postgraduate studentship. The review of this paper was coordinated by K. Molnar.

M. Hunukumbure is with the Fujitsu Laboratories of Europe Ltd., UB4 8FE, Middlesex U.K. (e-mail: Mythri.Hunukumbure@uk.fujitsu.com).

B. Allen is with the Department of Engineering Science, University of Oxford, OX1 2JD Oxford, U.K. (e-mail: Ben.Allen@iee.org).

M. A. Beach is with the Department of Electrical and Electronics Engineering, University of Bristol, BS8 1UB, Bristol, U.K. (e-mail: M.A.Beach@bristol.ac.uk).

Color versions of one or more of the figures in this paper are available online at http://ieeexplore.ieee.org.

Digital Object Identifier 10.1109/TVT.2007.904525

In this paper, the authors extend their previous code orthogonality analysis for a SISO link [2] to multiple-transmit-antenna [or multiple-input–single-output (MISO)] configurations. Two contrasting schemes, i.e., fixed beamforming and transmit diversity, are considered. Moreover, the quantification methodologies are applied to real measured channel data to obtain code orthogonality estimates for practical radio environments. Given the current interest in multiantenna technologies to enhance data throughput and reliability in HSDPA [1], this analysis acquires added significance. These code orthogonality estimates can be used in link-level cell capacity calculations, particularly to quantify intracell interference. The findings in this paper have also found some additional applications. A selection diversity scheme based on code orthogonality was proposed in [6] (for both SISO and MISO transmit links), which was shown to outperform the traditional received-signal-power-based selection criterion. The orthogonality quantifications were also used to estimate the multiaccess (broadcast channel) information theoretic capacities for the multiple-input multiple-output (MIMO)/MISO downlinks in [7].

This paper is organized as follows: In Section II, the code orthogonality quantification for the SISO links presented in [2] is reviewed. This methodology is extended to a fixed beamforming scenario in Section III. In addition, in Section III, this new quantification methodology is applied to real measured channel data, and code orthogonality values are calculated for urban-small-cell and urban-large-cell environments. The SISO derivations in [2] are extended to transmit diversity schemes in Section IV. Code orthogonality values are estimated for transmit diversity schemes in urban cells with measured channel data in this section. In addition, an empirical analysis into the inverse relationship between the code orthogonality and path diversity of the radio channels is presented here. Finally, the conclusions of this paper are presented in Section V.

II. Review of Code Orthogonality for SISO Systems

The code orthogonality quantification for SISO systems presented in [2] was based on deriving the signal-to-intracell-interference ratio (SIR) and mapping this to code orthogonality through a reference channel. The signal S and interference power I components for a code-division multiple-access downlink with orthogonal spreading have been derived by Adachi [8]. The S and I calculations in the following sections are adaptations from these basic SISO estimates. Citing from

[8],the instantaneous S and I at the output of an R-finger maximal-ratio-combining rake receiver are given by

$$S = (pg)^2 P \left(\sum_{m=1}^{R} |\xi_m|^2 \right)^2 \tag{1}$$

$$\begin{aligned} I &= I_{\mathrm{SLF}} + I_{\mathrm{MAI}} \\ &= (pg)P \left[\left(\sum_{m=1}^{R} \left(\sum_{l=1}^{m-1} 4\mathrm{Re}^2 \left[\xi_m^* \xi_l \right] \right) + |\xi_m|^2 \sum_{l=R}^{\infty} |\xi_l|^2 \right) \right. \\ &\qquad \left. + (C-1) \left(\sum_{m=1}^{R} |\xi_m|^2 \cdot \sum_{l=1}^{\infty} |\xi_l|^2 - \sum_{m=1}^{R} |\xi_m|^4 \right) \right]. \end{aligned} \tag{2}$$

The terms ξ_i denote the complex path gain for the ith selected channel path, pg is the processing gain, P is the average received signal power, and C is the number of interfering intracell users. The interference power consists of two components: 1) self-interference I_{SLF} and 2) multiaccess interference (MAI) I_{MAI}. I_{SLF} is the interference that is seen if only one user is active in the cell and caused by the nonzero autocorrelation properties of the OVSF code at nonzero lags. I_{MAI} is seen by the user when other users become active. The additive noise (additive white Gaussian noise) component has been ignored in (2), so measuring the SIR from an actual received signal is not possible. However, in coherent detection schemes, accurate channel estimates are available at the receiver. S and I, and subsequently SIR, can be calculated from these ξ_i channel gains, using (1) and (2).

It was shown in [2] that, when the uniform channel delay profile was used as the reference model, both the instantaneous SIR and instantaneous code orthogonality α can be related to the number of impulses N in the channel model as follows:

$$\mathrm{SIR} = \frac{pg}{C} \cdot \frac{N}{(N-1)} \tag{3}$$

$$\alpha = \frac{1}{N}. \tag{4}$$

For practical channel delay profiles, the SIR is calculated through (1) and (2), and an equivalent number of uniform impulses N (albeit fractional) is found with (3). The instantaneous code orthogonality α can be obtained from (4), once N is available.

III. Code Orthogonality With Fixed Beamforming

The code orthogonality for a fixed beamforming system (termed as α_{FXB}) is quantified in this section. In fixed beamforming, the M element transmit antenna array is fed with M mutually orthogonal weight vectors, which result in an M-fold orthogonal beam pattern [9]. The users are allocated to each beam on the basis of maximizing the received signal power, and they can be switched dynamically, depending on their movements [10]. The measured radio channel data used in Section III-B were recorded for static locations, which renders fixed beamforming more relevant to this analysis than a more complex adaptive beamforming scheme.

A. Quantification of α_{FXB}

When downlink beamforming is correctly applied, the SIR will improve due to two reasons. First, the spatial filtering effect will reduce the overall interference. Second, the delay spread and temporal variations of the channel will be reduced due to the suppression of multipaths with departure angles falling outside the main beam width. Only the second reason should contribute to an improvement (if any) in code orthogonality. To negate the SIR improvement due to the first reason in the reference channel model, a spatial filtering factor F is added to (3), i.e.,

$$\mathrm{SIR} = F \cdot \frac{pg}{C} \cdot \frac{N}{(N-1)}. \tag{5}$$

1) Calculation of Spatial Filtering Factor F: In an ideal beamforming model consisting of M "top hat"-type main beams and uniformly distributed interfering users, $F = M$. In practical beamforming systems, three loss factors diminish this gain, as identified in [10]. These loss factors are radiation loss L_{RAD}, azimuth spread loss L_{AS}, and cusping loss L_{CUSP}. L_{RAD} is determined by the radiation pattern of the antenna array. L_{AS} is based on the azimuth spread resulting from the transmitting signal's directions of departure (DoDs). L_{CUSP} accounts for the curvature of the radiation beam patterns at azimuth angles given by the DoDs. The following definitions are introduced to quantify these loss factors:

$$L_{\mathrm{RAD}} = \frac{\text{Outage power from allotted angular segment}}{\text{Total power in the radiation pattern}} \tag{6}$$

$$L_{\mathrm{AS}} = \frac{\text{Signal power outside allotted main beam}}{\text{Total signal power in the azimuth spread}} \tag{7}$$

$$\begin{aligned} L_{\mathrm{CUSP}} = &\sum_i (\text{Antenna gain of } i\text{th allotted beam}) \\ &* (\text{Power fraction of the } i\text{th DoD}). \end{aligned} \tag{8}$$

For a practical fixed beamforming scheme, the spatial filtering factor is conditioned by these three loss factors as

$$F = M \cdot (1 - L_{\mathrm{RAD}}) \cdot (1 - L_{\mathrm{CUSP}}) \cdot (1 - L_{\mathrm{AS}}). \tag{9}$$

2) Calculation of S and I Power Components: The M main beams in the fixed beamforming scheme will concurrently carry different users, depending on their azimuth locality. A given user will receive all the M beams with varying signal strengths, as the isolation among the beams is deteriorated due to sidelobes and multipath propagation. The allotted main beam for this user will carry the wanted signal and will also generate self-interference. Hence, (1) and the I_{SLF} part in (2) can be directly applied. The MAI will come from all M main

beams, making it necessary to change the I_{MAI} part in (2) as follows:

$$I_{\mathrm{MAI}} = pg \cdot \sum_{n=1}^{M} P_n C_n \times \left(\sum_{m=1}^{R} |\xi_{1,m}|^2 \cdot \sum_{l=1}^{\infty} |\xi_{n,l}|^2 - \sum_{m=1}^{R} |\xi_{1,m}|^2 \cdot |\xi_{n,m}|^2 \right) \quad (10)$$

where P_n is the received power (normalized to the signal power received from the allotted main beam), and C_n is the number of users for each of the M beams. Without loss of generality, it is assumed in (10) that the first main beam is allotted to the wanted user.

The actual SIR for a fixed beamforming scheme can be calculated with (1) and a modified version of (2), with I_{MAI} coming from (10). This instantaneous SIR is then substituted to (5) to obtain the number of impulses N in the reference channel model. Finally, α_{FXB} can be calculated using (4).

B. Calculation of α_{FXB} With Measured Channel Data

In simulating the fixed beamforming environment with real channel data, a basic requirement is to utilize a channel data set where the transmit antennas have been spaced apart by about half-wavelengths $(\lambda/2)$. Smaller antenna spacings lead to higher mutual coupling effects, and larger spacings generate undesirable grating lobes in the radiation pattern.

1) Single-Input Multiple-Output (SIMO) Field Trial Campaign: The radio channel data used in this analysis were excerpted from a single-transmit multiple-receive (or SIMO) field trial campaign conducted by the Centre for Communications Research (CCR), University of Bristol. A Medav RUSK channel sounder [11] was used in the trials, with a 20-MHz signal bandwidth centered on 1.91-GHz carrier frequency. The channel data were recorded in the frequency domain as path gains on 128 discrete frequency fingers.

The base station (BTS) was set up on three different university buildings (about 30 m above ground level) overlooking the city of Bristol. A dual-polarized $(\pm 45^\circ)$ antenna facet, with eight vertical subarray panels spaced apart by 0.54λ, was used as the receiving array at the base station. At the transmitting user end, an omnidirectional sleeve dipole with 2-dBi gain was employed. As the base station was mounted well above the local clutter around the user end, these radio environments can be classified as urban large cells and urban small cells. Twenty-seven static user locations were selected for measurement in the urban large cell, with a cell radius of about 1.5 km. For the urban-small-cell scenario, the transmissions were done at multiple static locations, which were repeated thrice for three base station sites. Thirty-six user locations within a cell radius of 0.5 km were realized for the urban small cell in this manner. These locations and the base station sites are illustrated in the map in Fig. 1.

Although the channel measurements were conducted in the uplink, channel reciprocity [12] allows these data files to be interpreted in the downlink. Only the $+45^\circ$ polarized channels are considered in the analysis, giving eight transmitting

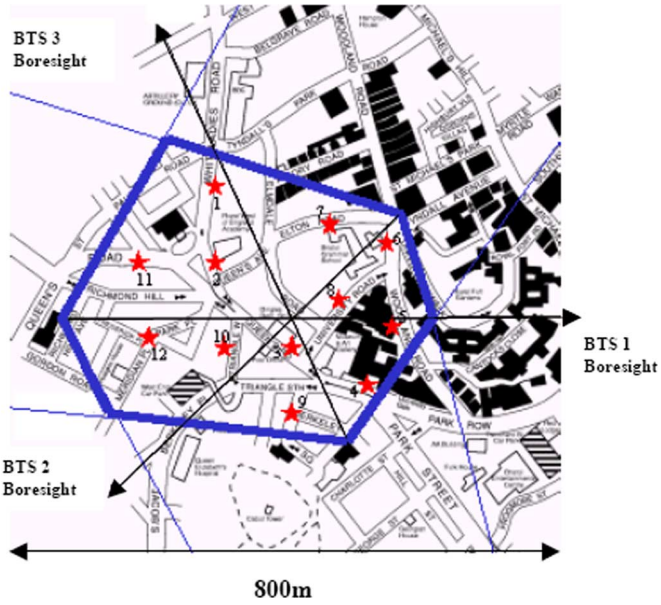

Fig. 1. Map of urban-small-cell measurement locations.

elements spaced apart by roughly 0.5λ as the fixed beamforming base stations. The top 5-MHz segment from the 20-MHz recorded data is chosen to be compatible with Universal Mobile Telecommunication System (UMTS) Terrestrial Radio Access (UTRA) standards. Full details of the trials and related propagation characteristics can be found in [13].

2) Method of Calculation and Results for α_{FXB}: The channel data recorded in the frequency domain were first converted to the delay domain by inverse fast Fourier transform. Each data file contained 100 instantaneous snapshots; hence, code orthogonality values were calculated for each snapshot and averaged to give a representative value per each measurement location.

In calculating α_{FXB}, processing gain pg was set to 64, and the number of users C was selected to be the same number of user locations. Although the channel sounding in user locations was carried out sequentially, the interference analysis was conducted with the assumption that the users were concurrently active. Both eight- and four-element fixed beamformers with 15° and 30° beam widths, respectively, were considered in the analysis. The number of users served by each main beam was assumed to be equal, providing a uniform azimuth distribution of active users. The cells were split into 120° sectors (as shown in Fig. 1), and the beamformers were implemented through 4×4 and 8×8 Butler matrices [14]. The signal DoDs from the base station sites, as required for the calculations in (7) and (8), were extracted using a 2-D ESPRIT algorithm [15]. The DoDs for signal multipaths within a 20-dB dynamic range (w.r.t. the peak signal) were detected and used in the calculations.

Estimates of α_{FXB} for both the urban-small-cell and urban-large-cell environments are shown in Figs. 2 and 3. These are the average α_{FXB} values, which are taken with the intention of illustrating the spatial variation of code orthogonality across typical urban cells. Code orthogonality values for single-element SISO channels are also added to aid comparisons.

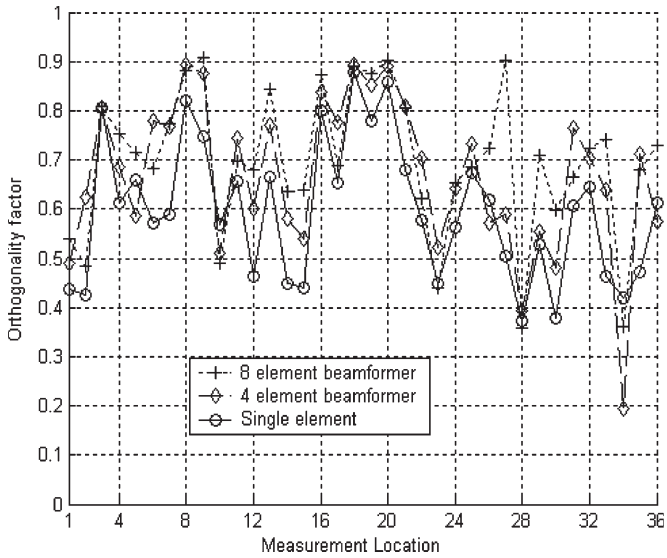

Fig. 2. Code orthogonality variations: urban-small-cell.

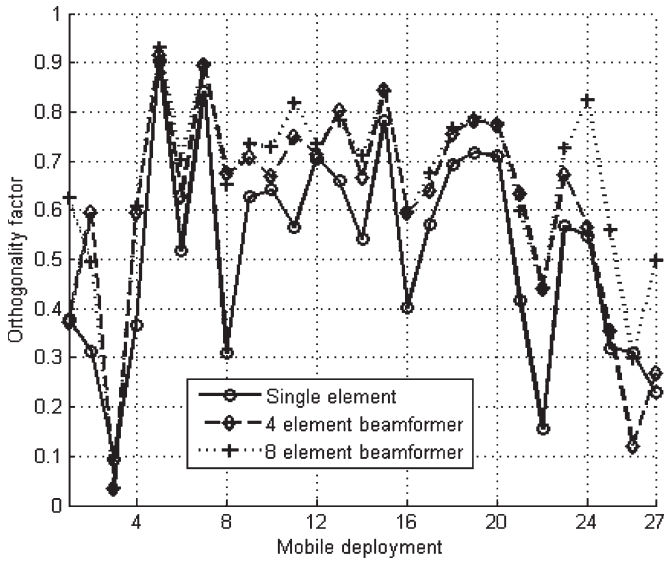

Fig. 3. Code orthogonality variations: urban-large-cell.

The mean value of α for SISO channels across the urban-small-cell locations is 0.596. This improves by 12.9% to 0.67 with the use of a four-element beamformer. With an eight-element beamformer, there is a 16.4% improvement of the mean α_{FXB} to 0.694. For the urban large cell, the mean value of α in the SISO system (0.557) improves by 15.3% to 0.64 with the four-element beamformer. With an eight-element beamformer, α_{FXB} increases by 24% to 0.69. In both cells, diminishing gains are indicated for increasing array sizes. For urban large cells, usually with more delay dispersion, the improvements with array processing are found to be greater. There is a significant variation of α_{FXB} values across a cell, depending on the locality of the user. The standard deviations of α_{FXB} are significant (0.14 in the small cell and 0.18 in the large cell) and should be included when quoting representative α_{FXB} values.

Interestingly, in a few mobile locations, fixed beamforming has deteriorated code orthogonality. The worst case can be seen at measurement location 34 in Fig. 2 (or BTS3 (location 10) in Fig. 1). Two channel delay profiles for this deployment—one with the SISO channel and the other taken with the four-element beamformer—are presented in Fig. 4.

The impulses in Fig. 4(b) have large magnitudes, and more importantly, three peaks are showing delay offsets. These offsets severely degrade the code orthogonality of the wanted user. The spatial resolution of the single-antenna channel by the four fixed main beams in this case has increased the overall delay spread. In a fixed beamforming system, there can be user locations that will experience degraded service. These are locations where users have a large azimuth angular spread or significant DoDs near the beam intersections.

IV. Code Orthogonality With Transmit Diversity

In transmit diversity schemes, the transmit signal is replicated through several transmit antennas, which produces a diversity gain. Transmit diversity implemented through space-time block coding (STBC) [16] is analyzed in this section. The low decoding complexity of STBC [16] and the ability to arbitrarily control the number of receive antennas are appealing features in terms of limiting the cost, complexity, and size of the handset. The orthogonality factor α_{TXD} is quantified for open-loop single-receive-antenna STBC schemes.

A. Quantification of α_{TXD}

In quantifying α_{TXD}, a similar approach as that in Section III is employed. First, the STBC code block is defined. Then, the signal and interference power components are calculated with equations adapted from (1) and (2) for schemes using this code block. Finally, the reference channel model is modified to suit the STBC scheme.

1) STBC Code Block: The STBC code blocks are orthogonal, which allows linear decoding [16]. However, for complex symbol code blocks with more than two transmit ports ($n_T > 2$), code rate R_c has to be compromised to maintain this orthogonality [16]. Scenarios with $n_T = 2$ and $n_T = 4$ are considered for this paper, and their code blocks X_2 and X_4 are denoted here (from [17]). The columns indicate the time slots, and the rows indicate the transmit ports. In X_4, R_c is reduced to 0.75 due to zero insertions. X_2 (originally proposed by Alamouti [18]) is the only complex code block to have $R_c = 1$, as shown in

$$X_2 = \begin{bmatrix} x_1 & -x_2^* \\ x_2 & x_1^* \end{bmatrix}$$

$$X_4 = \begin{bmatrix} x_1 & 0 & x_2 & -x_3 \\ 0 & x_1 & x_3^* & x_2^* \\ -x_2^* & -x_3 & x_1^* & 0 \\ x_3^* & -x_2 & 0 & x_1^* \end{bmatrix}. \tag{11}$$

2) Signal and Interference Power Components: The quantification of S and I terms in transmit diversity is shown for the $n_T = 2$ case for brevity; however, this can be easily extended to $n_T > 2$ cases. Under UTRA standards, the symbols going through multiple transmit ports are spread with the same OVSF

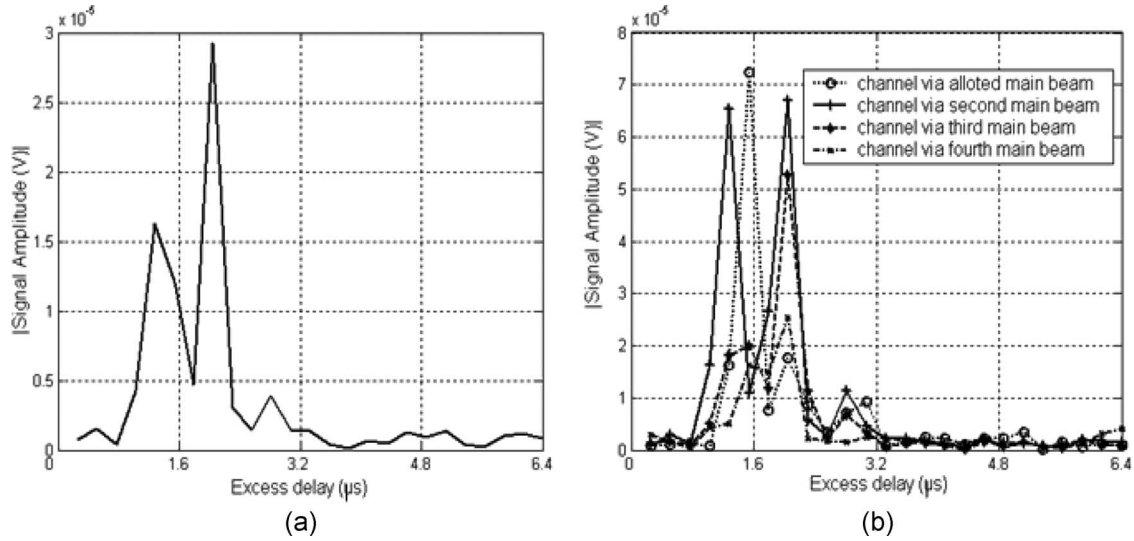

Fig. 4. Channel delay profiles: location 34 of urban-small-cell. (a) Single element. (b) Four-element beamformer.

code. For each of the R significant paths in the rake receiver, separate despreading and linear decoding (as in [18]) are carried out, and the signal paths are coherently combined. Signal power S for any of the symbols x_1 or x_2 can be expressed as

$$S = (pg)^2 \cdot P \cdot \left(\sum_{t=1}^{2} \sum_{m=1}^{R} |\xi_{t,m}|^2 \right)^2. \tag{12}$$

Channel gain $\xi_{t,m}$ denotes the mth significant path of the channel linking the tth transmit antenna to the single receive antenna. Although the transmitted power is halved (w.r.t. SISO), it effects both S and I, and P is unchanged.

Within n_T multipath dispersive radio channels, co-channel interference is produced by the delayed paths of the same channel (as for the SISO case). In addition, cross-channel interference is generated by the interaction of delayed paths of parallel radio channels. These interference powers combine linearly due to the linear decoding process at the receiver. When phase-shift keying (PSK) modulation is used, the absolute signal levels can be represented as $|x_1| = |x_2| = 1$. The four interference terms (two co-channel and two cross-channel terms) in the $n_T = 2$ case can be summed up without any scaling for PSK schemes. Thus, the I_{SLF} and I_{MAI} terms can be represented as

$$I_{\mathrm{SLF}} = pgP \cdot \sum_{s=1}^{2} \sum_{t=1}^{2} \sum_{m=1}^{R} \left(\sum_{l=1}^{m-1} 4\mathrm{Re}^2 \left[\xi_{s,m}^* \xi_{t,l} \right] \right) + |\xi_{s,m}|^2 \sum_{l=R}^{\infty} |\xi_{t,l}|^2 \tag{13}$$

$$I_{\mathrm{MAI}} = pgP \cdot (C-1) \left(\sum_{m=1}^{R} |\xi_{1,m}|^2 + \sum_{m=1}^{R} |\xi_{2,m}|^2 \right) \cdot \left(\sum_{\substack{l=1 \\ l \neq m}}^{\infty} |\xi_{1,l}|^2 + \sum_{\substack{l=1 \\ l \neq m}}^{\infty} |\xi_{2,l}|^2 \right). \tag{14}$$

It is of interest to compare (10) and (14). MAI in (10) was mitigated through spatial filtering and radio channel conditioning. However, in transmit diversity, all users occupy the available channels with equal power. There is no interference reduction or radio channel conditioning occurring in open-loop transmit diversity.

3) Adapting the Reference Channel Model: The uniform impulse channel model is again adapted for all MISO radio channels. In the case of $n_T = 2$, both S and I powers will increase four times, when compared to the SISO model. For the $n_T = 4$ case, some of the interference will not appear due to zero transmissions in X_4. Consequently, the interference power should be scaled by code rate R_c ($R_c = 1$ for $n_T = 2$) in the reference channel SIR, i.e.,

$$\mathrm{SIR} = \frac{pg}{R_c C} \cdot \frac{N}{(N-1)}. \tag{15}$$

The SIR derived for actual radio channels in (12)–(14) is used to find an equivalent N for uniform impulse reference channels from (15). This N (albeit fractional) is then related to the α_{TXD} of the selected transmit diversity scheme.

B. Calculation of α_{TXD} With Measured Channel Data

When modeling a transmit diversity environment, the transmit antenna ports need to be spatially (or through polarization) separated to invoke independent channel fading. In the MIMO channel measurement campaign described here, two dual-polar transmit antennas were sufficiently separated to produce good diversity gains.

1) MIMO Channel Measurement Campaign: An extensive 8×4 MIMO channel measurement campaign was conducted by the CCR, University of Bristol, again with the aid of a MIMO-enabled Medav RUSK BRI channel sounder [11]. The transmitting base station was set up on top of a five-storey university building, overlooking the Bristol city center. Two dual-polarized UMTS panel antennas spaced apart by 20λ were used at the transmit end. At the receive end, a uniform circular

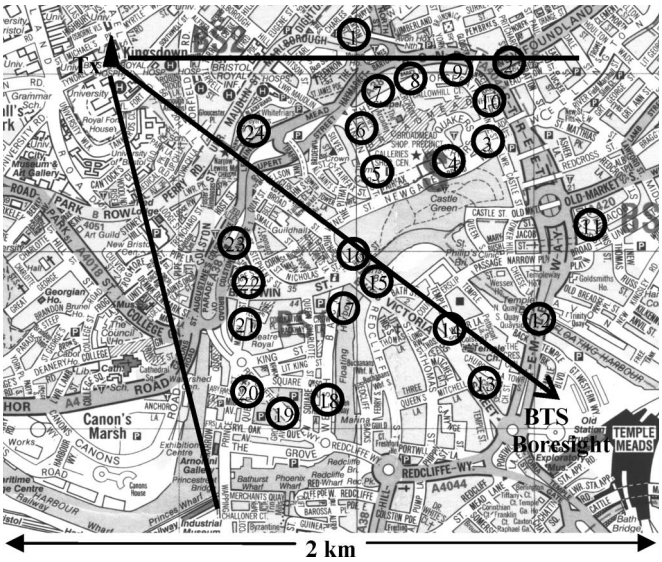

Fig. 5. Measurement locations for the MIMO campaign.

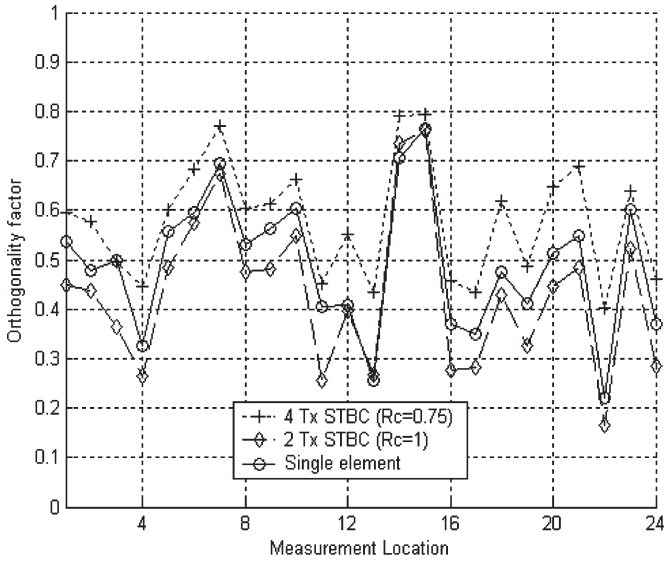

Fig. 6. Code orthogonality estimates for transmit diversity schemes.

array made up of eight monopoles was mounted on top of a car. The channel measurements were taken while the car was in motion.

Each measurement file contains 1024 snapshots spanning a 20.7-s duration. Within each snapshot, the 32 subchannels for the 8×4 MIMO configuration were recorded well within the channel coherence time, which makes them comparable to truly parallel MIMO channels. The measurements covered 24 predetermined locations. These locations are spread around in a radio cell with a 1.5-km radius. The base station site and the measurement locations are depicted in Fig. 5. A detailed description of the trials can be found in [19].

2) Calculations and Results of α_{TXD}: Code orthogonality values were calculated for $n_T = 2$ and $n_T = 4$ configurations by taking MISO channel data that link the first receive port with the transmit nodes. For $n_T = 2$, transmit nodes 1 and 3 with 20λ spatial separation were considered, whereas for $n_T = 4$, nodes with both spatial and polarization separations were included. For each measurement location, instantaneous α_{TXD} was calculated for the 1024 snapshots, and the mean value was chosen as the representative figure. Although the mean α_{TXD} values are highlighted in this analysis, the instantaneous α_{TXD} values are also useful in dynamic selection diversity schemes, as studied in [6].

The mean α_{TXD} estimates across the 24 measurement locations are plotted in Fig. 6, along with code orthogonality for reference SISO channels. The SISO channel linking transmit port 1 with receive port 1 is considered in $n_T = 1$ reference calculations.

The plots indicate that the code orthogonality has degraded in the $n_T = 2$ configuration, whereas in the $n_T = 4$ system, it has improved compared to the SISO channel. The mean value of α for the SISO channels is 0.491. This has degraded by 11.8% to 0.433 with the full-code-rate $n_T = 2$ system and has improved by 17.9% to 0.579 with the $n_T = 4$ configurations. The improvement in four-transmitter systems is due to the reduction in interference through the reduced code rate. It can also be noted that the 25% reduction in data throughput is only partially compensated by the improved code orthogonality. Code orthogonality values for all these configurations are found to significantly vary across the cell, as with the fixed beamforming scenario.

C. Impact of Channel Correlation on Code Orthogonality

A fundamental requirement in an effective diversity system is the sufficient decorrelation of the constituent radio channels [12]. However, channel decorrelation would have a detrimental effect on code orthogonality in transmit diversity schemes. Highly decorrelated channel profiles are likely to have their signal peaks offset in the delay domain, and this reduces code orthogonality. The impact of channel profile correlation on code orthogonality is analyzed here by modeling a simple relationship between these parameters.

A basic channel parameter that influences code orthogonality is the rms delay spread τ_{rms}. In channel delay profiles with an "orderly" distribution of significant paths, higher τ_{rms} would contribute to a reduction in α. This is demonstrated in (4), where a larger N for the uniform channel impulse response will yield a higher τ_{rms}. A log-linear relationship between α and τ_{rms} has been shown for exponentially decaying power delay profiles of SISO channels in [20]. In actual channel profiles, however, the significant paths are not orderly arranged. For a given value of τ_{rms}, different numbers of significant paths can be present with varying relative delays, and code orthogonality will change accordingly. This ambiguity between α and τ_{rms} can be reduced by incorporating the number of significant paths R into this log-linear relationship.

For transmit diversity composite channels, the channel profile correlation X_c can be defined as the correlation coefficient (ranging from 0 to 1) among the constituent channel delay profiles. Assuming better code orthogonality with higher channel correlation, the combined impact of X_c, τ_{rms}, and R on code orthogonality α_{TXD} is expressed as a log-linear

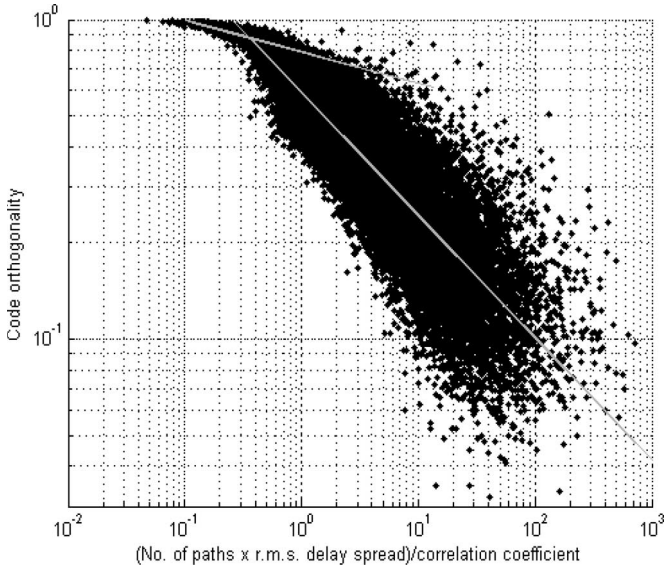

Fig. 7. Code orthogonality dependence on channel correlations.

relationship, which includes intercept and gradient coefficients a_0 and a_1, i.e.,

$$\log(\alpha_{\mathrm{TXD}}) = a_0 + a_1 \log\left(\frac{R\tau_{\mathrm{rms}}}{X_c}\right). \tag{16}$$

Using the same data set as in Section IV-B, the aforementioned modeled expression was tested for the $n_T = 2$ transmit diversity system. Channel data from all 24 locations in Fig. 5 were included in the sample. X_c was calculated for each instantaneous channel delay profile. The average τ_{rms} between the two instantaneous channels was also calculated. In addition, the number of active rake fingers is equal to R. The results are depicted as a scatter plot in Fig. 7.

The scatter plot indicates a significant distribution of values around the envisaged log-linear relationship. The ambiguity between α and τ_{rms} (although reduced with a defined number of R significant paths) plays a major role in causing these deviations. The dual-slope (two-step) log-linear function, as predicted for SISO channels in [20], can still be approximated with these results. A least squared curve fit (shown in gray) yielded gradient values of $a_1 = -0.1$ and $a_1 = -0.34$ for each of the two lines. The reason for having such a segmented function is the change in the number of active rake fingers [24]. In least squared curve fitting, the threshold was chosen as the point when R changed from $R = 1$ to $R > 1$. This implicit expression in (16) gives an indication of the inverse relationship between code orthogonality and channel decorrelation in transmit diversity schemes and is by no means a precise proof.

V. Conclusion

In this paper, novel quantifications for the code orthogonality are presented for UTRA-compliant fixed beamforming and transmit diversity schemes. These are extensions to the SISO channel derivation in [2] and verified with results that were obtained by evaluating measured channel data.

The analysis with measured channel data has shown code orthogonality to generally improve with fixed beamforming and with higher array sizes, bringing diminishing returns. With transmit diversity schemes based on STBC, the code rate has a direct impact on code orthogonality. With full-code-rate $n_T = 2$ systems code orthogonality degraded from the SISO reference case. With $n_T = 4$ systems with lower code rate and hence reduced interference, code orthogonality showed an improvement. However, this "superficial" improvement does not adequately compensate for the loss of data throughput. In general, it can be stated that the spatial conditioning of the radio channel through fixed beamforming has a positive impact on code orthogonality. However, with transmit diversity schemes, the combined multipath activity of the composite channels produces a negative impact on code orthogonality. The inverse relationship modeled between code orthogonality and spatial channel decorrelation (among other parameters) supports this observation.

An open question at this stage follows: "What other factors would influence the choice between beamforming and transmit diversity, and are they more critical than preserving code orthogonality?" Some useful insight is provided in [21] for a general cellular downlink, where factors such as fading correlation, angular spread, and handoff mechanisms are shown to contribute to this decision.

Acknowledgment

The authors would like to thank P. Karlsson, D. McNamara, S. E. Foo, C. M. Tan, C. Williams, and K. Stevens for their contributions during the measurements and data processing.

References

[1] H. Holma and A. Toskala, *WCDMA for UMTS–Radio Access for Third Generation Mobile Communications*, 3rd ed. Chichester, U.K.: Wiley, 2004.

[2] M. Hunukumbure, M. Beach, and B. Allen, "Downlink orthogonality factor in URTA-FDD systems," *Electron. Lett.*, vol. 38, no. 4, pp. 196–197, Feb. 2002.

[3] C. Passerini and G. Falciasecca, "Correlation between RMS delay spread and orthogonality in urban environments," *Electron. Lett.*, vol. 37, no. 6, pp. 384–385, Mar. 2001.

[4] N. B. Mehta, L. J. Greenstein, T. M. Willis, and Z. Kostic, "Analysis and results for the orthogonality factor in WCDMA downlinks," *IEEE Trans. Wireless Commun.*, vol. 2, no. 6, pp. 1138–1149, Nov. 2003.

[5] O. Awoniyi, N. B. Mehta, and L. J. Greenstein, "Characterizing the orthogonality factor for WCDMA downlinks," *IEEE Trans. Wireless Commun.*, vol. 2, no. 4, pp. 621–625, Jul. 2003.

[6] M. Hunukumbure, M. Beach, and J. Webber, "Utilizing code orthogonality information for interference suppression in UTRA downlink," in *Proc. 61st IEEE VTC—Spring*, Stockholm, Sweden, May/Jun. 2005, pp. 339–343.

[7] M. Hunukumbure and M. Beach, "MIMO capacity limits in a 3G WCDMA multi-access cell," in *Proc. IEE 3G Conf.*, London, U.K., Oct. 2004, pp. 98–102.

[8] F. Adachi, "Effects of orthogonal spreading and rake combining on DS-CDMA forward link mobile radio," *IEICE Trans. Commun.*, vol. E80-B, no. 11, pp. 1703–1712, Nov. 1997.

[9] B. Allen and M. Gavami, *Adaptive Array Systems: Fundamentals and Applications*. Chichester, U.K.: Wiley, 2005.

[10] B. Allen and M. Beach, "On the analysis of switched-beam antennas for the W-CDMA downlink," *IEEE Trans. Veh. Technol.*, vol. 53, no. 3, pp. 569–578, May 2004.

[11] Medav GmbH. [Online]. Available: http://www.channelsounder.de

[12] J. D. Parsons, *The Mobile Radio Propagation Channel*, 2nd ed. Chichester, U.K.: Wiley, 2000.
[13] B. Allen, J. Webber, P. Karlsson, and M. Beach, "UMTS spatio temporal propagation trial results," in *Proc. 11th IEE ICAP Conf.*, Apr. 2001, pp. 497–501.
[14] J. L. Butler and R. Lowe, "Beam forming matrix simplifies design of electronically scanned antennas," *Electron. Des.*, vol. 9, no. 8, pp. 170–173, Apr. 12, 1961.
[15] M. Haardt, "Efficient one-, two-, and multidimensional high-resolution array signal processing," Ph.D. dissertation, Technische Universität München, Munich, Germany, 1996.
[16] V. Tarokh, H. Jafarkhani, and A. R. Calderbank, "Space-time block codes from orthogonal designs," *IEEE Trans. Inf. Theory*, vol. 45, no. 5, pp. 1456–1467, Jul. 1999.
[17] E. G. Larsson and P. Stoica, *Space Time Block Coding for Wireless Communications*. Cambridge, U.K.: Cambridge Univ. Press, 2003.
[18] S. M. Alamouti, "A simple transmit diversity technique for wireless communications," *IEEE J. Sel. Areas Commun.*, vol. 16, no. 8, pp. 1451–1458, Oct. 1998.
[19] M. Hunukumbure, M. Beach, C. Williams, and S. E. Foo, "MIMO capacity limits in outdoor 3G systems," in *Proc. 13th IST Summit Mobile Commun.*, Lyons, France, Jun. 2004.
[20] K. I. Pedersen and P. E. Mogensen, "The downlink code orthogonality factors influence on WCDMA system performance," in *Proc. 56th IEEE VTC—Fall*, Vancouver, BC, Canada, Sep. 2002, pp. 2061–2065.
[21] B. Friedlander and S. Scherzer, "Beamforming versus transmit diversity in the downlink of a cellular communications system," *IEEE Trans. Veh. Technol.*, vol. 53, no. 4, pp. 1023–1034, Jul. 2004.

Mythri Hunukumbure received the B.Sc. degree in electronic and telecommunications engineering from the University of Moratuwa, Moratuwa, Sri Lanka, in 1998 and the M.Sc. and Ph.D. degrees from the University of Bristol, Bristol, U.K.

He is currently a Research Engineer with Fujitsu Laboratories of Europe Ltd., Middlesex, U.K. He has been actively involved in the European COST273, IST-Saturn, and Mobile VCE research programs and now with 4G WiMAX-related research at Fujitsu. His research interests include the appraisal of code orthogonality and space-time signal processing technology to 3G mobile systems.

Ben Allen (SM'05) received the Ph.D. degree from the University of Bristol, Bristol, U.K., in 2001.

In 2002, he joined Tait Electronics Ltd., Christchurch, New Zealand, before becoming a Research Fellow at the Centre for Telecommunications Research, King's College London, London, U.K. In 2003, he became the Member of the Academic Staff. In 2005, he joined the Department of Engineering Science, University of Oxford, Oxford, U.K. He has published widely in the area of wireless systems, including his latest book *Ultra Wideband Antennas and Propagation for Communications, Radar and Imaging* (Wiley, 2006).

Dr. Allen is a Fellow of the Institution of Engineering and Technology (IET) Antennas and Propagation Professional Network Executive Committee and the Editorial Board of the *IET Microwaves, Antennas and Propagation Journal*. He was the recipient of the IET J. Langham Thompson Premium.

Mark A. Beach (A'90–M'06) received the Ph.D. degree, for research addressing the application of smart antennas to Global Positioning System, from the University of Bristol, Bristol, U.K., in 1989.

He subsequently joined the University of Bristol as a Member of the Academic Staff. He is also the U.K. National Representative on the EU COST 2100 action, and in August 2006, he was appointed as Head of the Department of Electrical and Electronic Engineering, University of Bristol. His interest in smart antenna techniques has continued with the application of dual-array techniques, or multiple-input–multiple-output (MIMO) architectures, to high-performance wireless networks. In particular, he has conducted research in the area of double-directional channel measurements and analysis as well as the practical characterization channel of MIMO using realistic user devices. He also has active interest in analog RF technologies for cognitive radio and spectrum sharing, and leads this theme within the MobileVCE Delivery Efficiency Research Programme.